Materials and Design 184 (2019) 108176

Contents lists available at ScienceDirect

Materials and Design

journal homepage: www.elsevier.com/locate/matdes

Smart and robust electrospun fabrics of piezoelectric polymer nanocomposite for self-powering electronic textiles

Deepalekshmi Ponnamma [a,*], Hemalatha Parangusan [a], Aisha Tanvir [b], Mariam Al Ali AlMa'adeed [c]

[a] Center for Advanced Materials, Qatar University, P O Box 2713, Doha, Qatar
[b] Advanced Composites Centre for Science and Innovation (ACCIS), Department of Aerospace Engineering, University of Bristol, Bristol BS8 1TR, UK
[c] Materials Science & Technology Program (MATS), College of Arts & Sciences, Qatar University, Doha 2713, Qatar

HIGHLIGHTS

- Smart PVDF-HFP nanocomposite, useful as electronic textile clothing, was made by electrospinning.
- PVDF/nanocellulose/Fe-doped ZnO hybrid nanocomposite showed a maximum output voltage of 12 V.
- Current density for the ferroelectric nanogenerator was enhanced 2.3 times compared to PVDF-HFP.
- Piezoelectric responses of the nanogenerator to various movements were investigated.

GRAPHICAL ABSTRACT

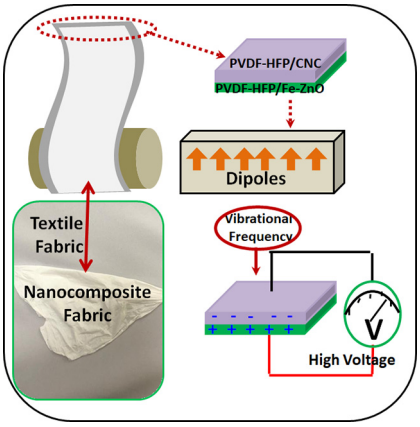

ARTICLE INFO

Article history:
Received 6 June 2019
Received in revised form 30 August 2019
Accepted 31 August 2019
Available online 31 August 2019

Keywords:
Electronic textiles
Nanogenerators
Dielectrics
Nanofabrics

ABSTRACT

The present work designs a piezoelectric nanogenerator (PENG) based on the electrospun nanofibers of the piezoelectric polymer, polyvinylidene fluoride hexafluoropropylene (PVDF-HFP), by uniformly drawing the spun membranes containing cellulose nanocrystals (CNC, 2 wt%) and the Fe-doped nano ZnO (2 wt%). The hybrid nanocomposite fibers were made in double layers, with CNC/PVDF-HFP composite on one side and the Fe-doped ZnO/PVDF-HFP on the other side. This ferroelectric polymer composite exhibited maximum peak-to-peak output voltage of 12 V with a current density, 1.9 μAcm^{-2}, which are respectively higher by 60 and 2.3 times compared to the neat polymer fibers. The PENG is tested for its energy harvesting ability by exposing it to different environments such as ultrasound vibrations and human body movements during hand tapping, elbow movements and by attaching with the textile fabrics. While the finger tapping generated peak-to-peak output voltage of 6.5 V, elbow movements resulted in 5.5 V generation. In all sorts of movements, the nanogenerator shows good output performance indicating its compatibility with textile materials. The mechanical properties, breakdown strength and dielectric properties of the material are also in accordance with its possible applications in wearable electronic textiles.

* Corresponding author.
E-mail address: deepalekshmi@qu.edu.qa (D. Ponnamma).

https://doi.org/10.1016/j.matdes.2019.108176

1. Introduction

Portable electronic devices are highly needed for many industrial applications and they are essential elements in Internet of Things (IoT) technology [1,2]. The wearable electronic chips and rollup displays, possessing features such as lightweight, biocompatibility and environmental friendliness are deeply investigated nowadays for their ability to harvest energy [3–5]. Moreover, bioinspired electronic skin sensors mimicking human skin are developed for health care monitoring as well as for robotic applications [6]. Ability of mechanical energy harvesting for such flexible and wearable devices are highly in demand since they can be easily connected with human body movements, like talking and walking [7–10]. The nanogenerators made for such purposes work mainly based on the piezoelectric effect and electrical signals are generated as output responses [11,12].

Among the various available piezoelectric materials, the inorganic ceramics such as lead zirconate titanate (PZT), lead magnesium niobate lead titanate (PMN-PT), barium titanate ($BaTiO_3$) etc. exhibit good level of piezo response, however their brittle nature restricts their application in flexible and wearable technology [13]. In this situation, piezoelectric nanogenerators (PENG) are made by embedding ceramic nanofillers of high piezoelectric coefficients in various flexible polymeric media of good processability [14–16]. The simple structure, relatively smaller size and long-term stability of the PENGs enable them to harvest energy by utilizing abundant energy sources from our living surroundings even from the sound waves, flowing air, mechanical impacts etc. [17–19]. Ferroelectric ceramic/polymer composites based on polyvinylidene fluoride (PVDF) [20] and its copolymers with trifluoroethylene [P(VDF-TrFE)] [21] and hexafluoropropylene [P(VDF-HFP)] [22,23] are widely reported for their piezoelectricity [24,25]. $BaTiO_3$ in 30 vol%, enhanced the dielectric constant of PVDF by 15%, when it is fabricated as core-shell structured polymeric nanocomposite [20]. At the same time, the ferroelectric $BaTiO_3$ particles combined with hexagonal boron nitride showed a dielectric constant of 45 and piezoelectric voltage of 2.4 V in its PVDF-HFP nanocomposite [24]. However, in the case of ceramic polymer composites, the applied mechanical stress is hard to reach within the ceramic piezoelectric particles since the major polymeric phase protects them. This causes inefficient load transfers between ceramic-polymer interface and the ceramic particles can't be fully exploited for their piezoelectric responses [2,16]. In addition, the nature of dispersion or aggregating tendency of particles again reduces the stress transfer efficiency [26].

Designing proper architecture by making use of doping/functionalization or filler synergy for minimizing the stress transfer effect and to enhance the piezo voltages are reported [1,27]. Dutta et al. were able to fabricate silica coated nickel oxide nanoparticles and its composite with PVDF and the nanocomposite PENG developed by them exhibited a maximum output voltage of 53 V with 685 W/m^3 power density [1]. This particular material was able to light up commercial LEDs with gentle human tapping in addition to its possible use in electronic skin sensors. On the other hand, multiple source energy harvesting system based on ZnO embedded flexible paper matrix showed the capability for producing upto 80 mV output voltage (power of 50 μWcm^{-2}) [27]. Apart from this, numerous reports have come out about the possible use of semiconducting ZnO in manipulating PVDF and/or [P(VDF-HFP)] based PENGs [11,14,28,29].

Since ZnO dispersion is not very effective to completely harvest the benefits of fabricated PENGs, doped ZnO with better dispersability in polymers are often used to make flexible PENGs [11,14]. Cellulose is notable to form crystalline fibers, and its significance to strengthen the bonding with compounding material through hydrogen bonding is rather significant [30]. This biocompatible and low cost material has lower coefficient of thermal expansion, making it sustainable for the designed device's thermal and mechanical stability. For instance, cellulose templates were utilized to design 3D piezo ceramic skeleton of Samarium doped $Pb(Mg_{1/3}Nb_{2/3})O_3$-$PbTiO_3$ (Sm-PMN-PT) with ultrahigh piezoelectric voltage of 60 V and power 11.5 μWcm^{-2} [2]. Cellulose nanocrystals (CNC) were also utilized as filler particles for PVDF and the so developed CNC/PVDF composite was able to charge a 33-μF capacitor over 6 V and light up commercial LED for more than 30 s [31]. Comparatively, Rajala et al. achieved good piezoelectric responses for the self-standing native cellulose nanofibril/PVDF films [32] and proved the potential application of such material in fabricating portable electronic devices.

By considering the major facts of preferably higher filler dispersability and lower interfacial tensions in a polymer nanocomposite, it is important to exploit the piezoelectric performances of modified nanoparticles, when embedded within a polymer. In this work, piezoelectric properties of CNC and ZnO nanomaterials are fully exploited by doping the latter with Iron ions and thus successfully embedding the hybrid fillers in [P(VDF-HFP)] medium. Doping with iron regulates the average crystallite size of ZnO [33] and the interstitial Fe ions present as surface charges contributes towards the ferroelectric property [34]. Since crystallinity and ferromagnetism are two important parameters to regulate the piezoelectricity, Fe-doping was practiced here for the ZnO. Electrospinning is used for the sample preparation since it generates nanofibrous mats with aligned [P(VDF-HFP)] dipoles. Fiber drawing is applied to design the smart PENG fiber mat by successively depositing Fe-ZnO and CNC in subsequent layers. The combined influence of hybrid filler effect, crystallinity regulation and filler piezo effect was investigated on the background of uniform fiber drawing process. The final nanocomposite mat of around 0.1 g weight generates an output (peak to peak) voltage of 12 V with low current density (1.9 μAcm^{-2}). The application of such nanocomposite fibers in designing smart electronic clothing capable of power generation is well demonstrated here.

2. Experimental details

2.1. Materials

The ferroelectric polymer [P(VDF-HFP)] with molecular weight M_w = 400,000 along with the solvents- N,N dimethylformamide (DMF) and Acetone were purchased from Sigma Aldrich. Cellulose microfibers, ammonium per sulphate (APS) and NaOH, were used for the synthesis of CNC and zinc acetate dihydrate [$Zn(CH_3COO)_2.2H_2O$], monoethanolamine or MEA [C_2H_7NO], polyethylene glycol (PEG), ethanol and iron chloride were used for the synthesis of Fe-doped ZnO. All these chemicals were commercially obtained from Aldrich, and were used as such without any purification.

2.2. Synthesis of CNC

A reported one-step method was adopted for the synthesis of CNC [35], by which the required amount of cellulose microfibers was made in to a suspension in 1 M APS solution by vigorously stirring at 60 °C for 16 h. After centrifugation at 10,000 rpm for 10 min, the obtained pellet was repeatedly washed with deionized water until the pH becomes 5. Ultrasonication of this cellulose nanofiber pellet breaks the nanofiber agglomerates and this was followed by neutralization with 1 M NaOH and lyophilization, to obtain the final CNC powder [36].

2.3. Synthesis of Fe-doped ZnO

The Fe-doped ZnO was prepared by our previously reported hydrothermal procedure [37]. Briefly, about 0.5 g PEG surfactant was added to a mixture of zinc acetate and iron chloride in 50 ml deionized water by maintaining the Zn/Fe ratio as 0.10. After proper stirring, 3 ml MEA was added and the whole mixture was kept in an autoclave at 140 °C for 15 min. When the reaction was completed, the precipitate was washed

with double distilled water and ethanol, dried for 12 h at 80 °C and annealed for 2 h at 400 °C.

2.4. Fabrication of electrospun fiber mats of polymer nanocomposite

10% solution of the polymer, [P(VDF-HFP)] was prepared in a 1:1 solvent mixture of DMF and Acetone by stirring at 70 °C for 3 h. Separate dispersions of the CNC and Fe-doped ZnO nanomaterials were made in the same solvent mixture at 2 wt% by bath sonication for 2 h. Later, the filler dispersions were mixed with the [P(VDF-HFP)] solutions by magnetic stirring overnight, to make the "polymer nanocomposite" suspensions of [P(VDF-HFP)]/Fe-ZnO and [P(VDF-HFP)]-CNC for electrospinning. Spinning the solutions were done by the established protocol for the similar polymeric system containing Co-doped ZnO nanomaterials [11], and the both solutions of [P(VDF-HFP)]/Fe-ZnO and [P(VDF-HFP)]/CNC were spun one above the other on a rotating collector and drawn out. Individual nanocomposite membranes were also fabricated by spinning [P(VDF-HFP)]/Fe-ZnO and [P(VDF-HFP)]/CNC suspensions separately in double layers, apart from the neat polymer.

2.5. Characterization methods

To investigate the morphological features of both nanomaterials and nanocomposite fibers, scanning electron microscope (Nova Nano SEM 450) and transmission electron microscope (TEM) (Phillips CM 12) were used. While the structural features were addressed by X-ray diffractometer (Empyrean, Panalytical, UK) during 2θ, 10° to 70°, piezoelectric properties were tested by using an assembled experimental set up [11,14]. The set up included a chain of components such as frequency generator, amplifier, vibrating shaker, resistor box and data acquisition system. Depending on the vibration frequency, the weight (2.5 N) placed on the silver electroded sample surface impart a compressive strain within the sample, and insist mechanical movement of dipoles. This creates voltage signals, which can be monitored from the National Instruments software. The mechanical properties of the samples were checked using the universal testing machine (Lloyd 1KN LF Plus, AMETEK, Inc., Bognor Regis, UK) at 5 mm/min and the dielectric properties were recorded using broadband dielectric spectroscope GMbH concept 40 (NOVO control Technologies, Germany).

3. Results and discussion

The fabrication processes involved in this study are schematically represented in Fig. 1. The spherical ZnO nanoparticles are modified to ZnO nanostars during the hydrothermal synthesis of Fe-doped ZnO as represented in Fig. 1a. The typical star like appearance of the Fe-ZnO is clear from the TEM image in Fig. 1b. According to Ostwald ripening mechanism, the nanorods formed during the synthesis arrange in specific fashion to form nanostar in presence of the MEA seed nuclei. The average base width of the hands of the Fe-ZnO star was about 44 nm with a hand-to-hand distance of 1.2 μm. In addition, the star formation and phase purity of Fe-ZnO was investigated by the XRD image provided as Supporting Information Fig. S1a. From the previously reported study of Fe-ZnO by our research group [37], the average crystallite size calculated from XRD for Fe-ZnO was 19 nm. In fact, the smaller crystallite size contributes to better piezoelectric performance. While the Fe-ZnO was prepared by hydrothermal reaction, CNC was obtained by hydrolysis process as demonstrated in Fig. 1c. The nanofibrils of CNC are visible as seen in the TEM image (Fig. 1d). Moreover, the XRD image in the Supporting Information Fig. S1b shows the presence of (101), (002) and (004) crystal planes.

Electrospinning method was employed to draw the fiber mats of [P(VDF-HFP)] nanocomposites containing Fe-ZnO and CNC nanomaterials. The thickness of the fiber was maintained as 0.5 μm for all samples of neat [P(VDF-HFP)], [P(VDF-HFP)]/Fe-ZnO, [P(VDF-HFP)]/CNC and for the hybrid nano membrane. Hereafter all these four samples studied are respectively denoted as PHP, P-FZ, P-CN and P-FC. The specific significance of this method lays in: (i) the very high aspect ratio of the nanomaterials as well as the nanocomposite fibers, (ii) the lower loading percentage of the nanomaterials and (iii) the lightweight of the fabricated fiber mat, an important merit for integration in wearable electronics.

Fig. 2 further analyses the crystalline regions and the lattice points of the nanomaterials and the aspect ratio of the nanofibers. In the case of CNC, the hydroxyl groups and the oxygen atoms in the skeleton cause the formation of hydrogen bonds and thus forms a highly ordered crystalline domain [38]. The synthesis process from the cellulose microfibril precursor enhanced the crystalline regions in the CNC as confirmed from the XRD image (Supporting Information Fig. S1b). The well-defined crystalline structure shown in Fig. 2a calculates a lattice spacing

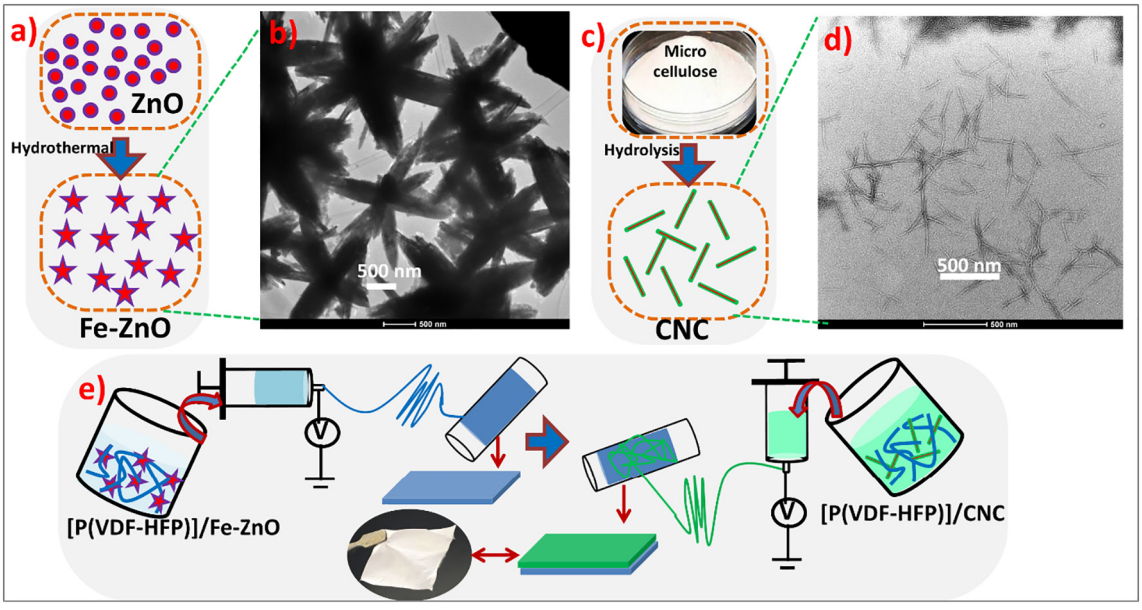

Fig. 1. a) Schematic representation of Fe-ZnO synthesis b) TEM image for Fe-ZnO c) synthesis process for the CNC d) TEM image for CNC e) schematic for the fabrication of electrospun fiber mat.

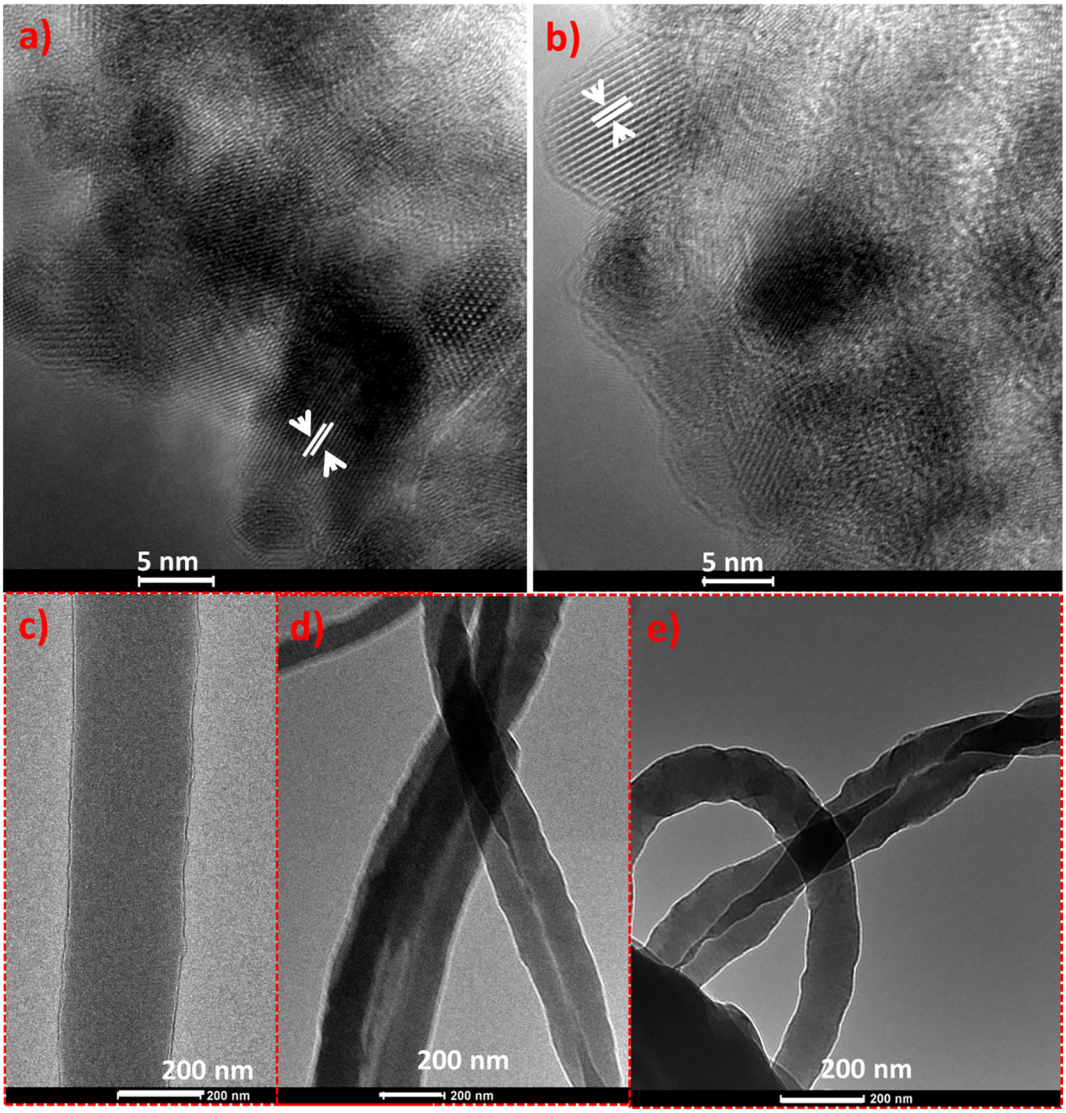

Fig. 2. HRTEM images of a) CNC b) Fe-ZnO; TEM images of c) PHP d) P-FZ e) P-CN nanocomposites.

of 0.5 nm for the CNC. The hydrothermally synthesized ZnO forms one-dimensional structures along its c-axis because of the alternate Zn^{2+} and OH^{-} ions in the skeleton. Whereas doping creates 2D structures, as dopant ions in the solution bind to Zn^{2+} terminated polar face, and decreases the ZnO growth rate along the c-axis. Crystal structure and composition of the fillers are further analyzed with HRTEM images, which shows the single crystal structure as represented in Fig. 2b. Lattice fringe spacing is observed as 0.28 nm corresponding to the ZnO (001) planar distance. This evidences for the crystalline nature of both the filler particles used.

Electrospun fibers were also investigated for its morphology and aspect ratio as represented in Fig. 2c–e. The [P(VDF-HFP)] nanofiber showed a diameter of 272 nm whereas the incorporation of nanoparticles decreased the fiber diameter. In the case of [P(VDF-HFP)]/Fe-ZnO nanocomposite, the average value obtained was 175 nm and for [P(VDF-HFP)]/CNC, the average diameter was 114 nm. In addition, the fibers obtained were twisted and interwoven in the case of both Fe-ZnO and CNC composites when compared to the segregated fiber morphology of the neat polymer. This confirms the increased length of the individual polymer fibers and thus the aspect ratio. This is a good sign as far as the piezoelectric fabric application is concerned so that the fabricated nanofibers can be compatible with the normal textile fibers. In addition, the spun fibers possess lightweight too. The crystallinity information for all the samples are illustrated by the FTIR and XRD results in the supporting information, Fig. S2. It is also in correlation with the DSC results (Fig. S3) as indicated in Table S1.

Designing flexible nanogenerators from the piezoelectric composite fibers generally involve many steps. Here, the piezoelectric hybrid fibers containing Fe-ZnO and CNC nanomaterials are silver electroded on both sides with connecting wires and thereafter spin coated with PDMS to make a nanogenerator. Fig. 3a schematically represents the major steps involved in the nanogenerator fabrication. The PDMS coated nanogenerator was properly covered as shown in Fig. 3a. The photographs also show the delicate nature of the fibers, its lightweight and flexibility. After fabricating the PENG, it was tested for the piezoelectric performance by evaluating the output voltage and current signals. When a specific weight of 2.5 N was placed on the sample kept on the top of a vibrating shaker, compressive mechanical deformation was imparted on the sample, generating electrical signals. By varying the vibrating frequency from 20 to 50 Hz, the output voltage generation was recorded for all samples. The results obtained for the hybrid sample over a range of vibrating frequencies are demonstrated in Fig. 3b. The maximum output voltages generated for all the samples at a specific vibrational frequency (45 Hz) are also compared in Fig. 3c. In addition, the output current values were also checked for all the samples, and the result obtained for the P-FC is shown in Fig. 3d. Among all the samples the

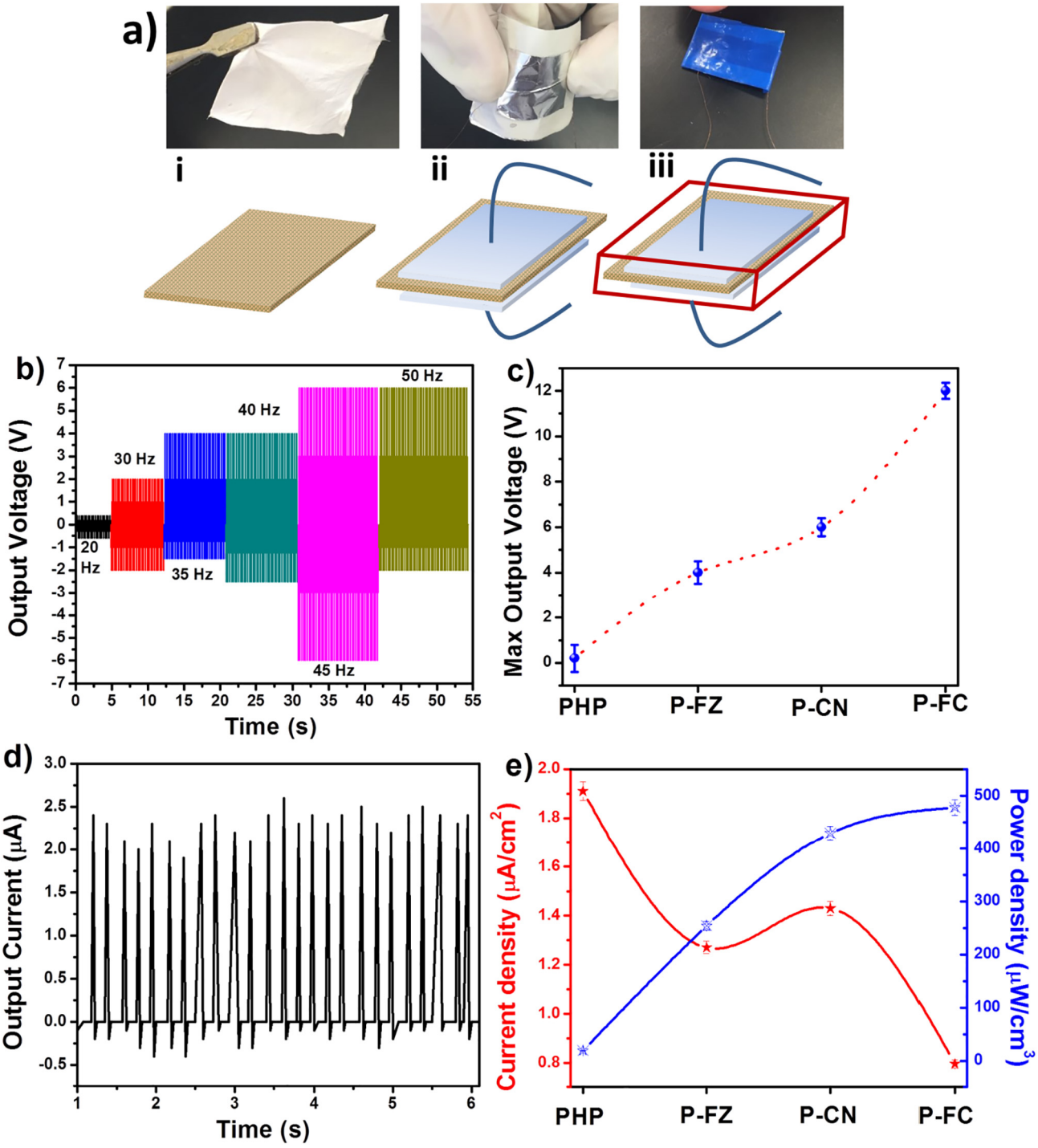

Fig. 3. a) Representation of the PENG fabrication, b) variation in output voltage with time for the hybrid composite P-FC at different vibrating frequencies, c) Maximum output voltages for all samples, d) variation in output current with time for P-FC at 45 Hz vibrating frequency and e) current density and power density for all samples.

P-FC showed a maximum output voltage of 12 V (Fig. 3c) with current density 1.9 μAcm^{-2} (Fig. 3e).

The external electric field during electrospinning process aligns the filler domains in a typical piezoelectric polymer nanocomposite so that piezo voltage is enhanced in specific direction. In the absence of fillers, the output signal is negligible, and the response only comes from the piezoelectric activity of the polymer and its dipoles.

It is notable that the filler concentration enhances the piezoelectric voltage [11]. However, a constant amount of 2 wt% is used here based on our previous works on doped ZnO filled polymer systems [11,14]. Such smaller filler concentration leaves the possibility of enhanced dielectric constant, which can weaken the electromechanical coupling effect. The device's output performance is measured in terms of open circuit voltage and short circuit current. During the switching polarity test, negative pulses from reverse connection and positive pulses from pressing are formed with average output voltage and current density at similar magnitude. This rule out the possibility of artifacts from the measuring system and triboelectricity [39]. The efficiency of the PENG is calculated in terms of the power density, which is represented in the Fig. 3e along with the current density for various samples. The

instantaneous power density is in accordance with the following relation,

$$\text{Power Density} = \frac{Power}{volume} = \frac{VXI}{AreaXthickness} \quad (1)$$

where V is the voltage and I the current across specific load resistance (1 MΩ). Here the maximum power density obtained is 490 μW/cm^3 for the hybrid spun membrane containing both Fe-ZnO and CNC nanomaterials. This value is comparable to similar reports on PENGs made of PVDF and its copolymers. While Mao et al. [40] obtained the maximum power density of 0.15 mW/cm^3 for PVDF thin film PENG, Bhavanasi et al. [41] achieved 4.41 μW/cm^2 for the bilayer films of PVDF-TrFE and graphene oxide.

In order to have a direct understanding of the PENG's energy harvesting efficiency, the piezoelectric output voltage generated was monitored by imparting various strains on it. Fig. 4 demonstrates the output voltages generated during human finger tapping, ultrasonication (frequency of 20 kHz) and elbow movements (upto 90° movement). The polarity switching test was done to verify the output signal obtained from the PENG itself. Similar peaks were observed both in the forward and reverse directions during tapping and releasing (Fig. 4a).

The PENG is kept in ultrasonication bath as shown in Fig. 4b, to monitor the efficiency of energy conversion by ultrasonic waves. The vibrations were given in specific time intervals and repeatability and recyclability for the same sample were also investigated. It is found that the output voltage becomes 2 V, during ultrasonic sound vibration. This observation evidences for the capability of sound waves in imparting mechanical deformation by changing the dipole alignment within the nanocomposite. During the elbow movement, as shown in the Fig. 4c, the PENG undergoes a bending movement and upon bending the PENG, tensile strain along with compressive deformation (Poisson effect) is induced within it. The device performance upon the various stimulations is demonstrated in the Supplementary video. It is established from the morphology that both Fe-ZnO and CNC are bound firmly within the network of polymer dipoles. As the ZnO nanostars are larger than the CNC (higher aspect ratio and the lattice space as well), the effective external strain transfers to Fe-ZnO and generates piezo potential [42]. In fact, electrospinning creates lightweight and durable fibers with better elongation and less brittleness compared to the solvent casted film. Such electrospun non-woven mats contain entangled polymer chains with clear porosity, and the porosity reduces the polymer cohesive force and voids allowing relaxation of polymer chains [43]. Generally, the piezoelectricity of a material depends on change in polarization density and dipole moment formation within it. Here, in the hybrid composite membrane, both Fe-doped ZnO and CNC nanomaterials play significant role in enhancing the piezo potential. The CNC synthesized by deconstructing fibrillary cellulose, is notable for its crystallinity, alignment and dipolar orientation [44]. In addition, the presence of Fe-ZnO particles, creates two strains within the polymer nanocomposite membrane. When the spun membrane vibrates, the nanostars (Fe-ZnO) and nanofibrils (CNC) rub each other along with the vibrations of individual particles (nanostar-nanostar and nanostar-nanofibril) [27].

The output voltage result while attaching the PENG to the cloth is demonstrated in Fig. 4d. The fiber nanocomposite membrane before designing the PENG is attached to the cloth as shown in the figure inset. This ensures the compatibility of the spun mat in designing electronic textiles. Gentle folding movements of the cloth generated an output voltage of 1.1 V, that evidences for the possibility of manufacturing

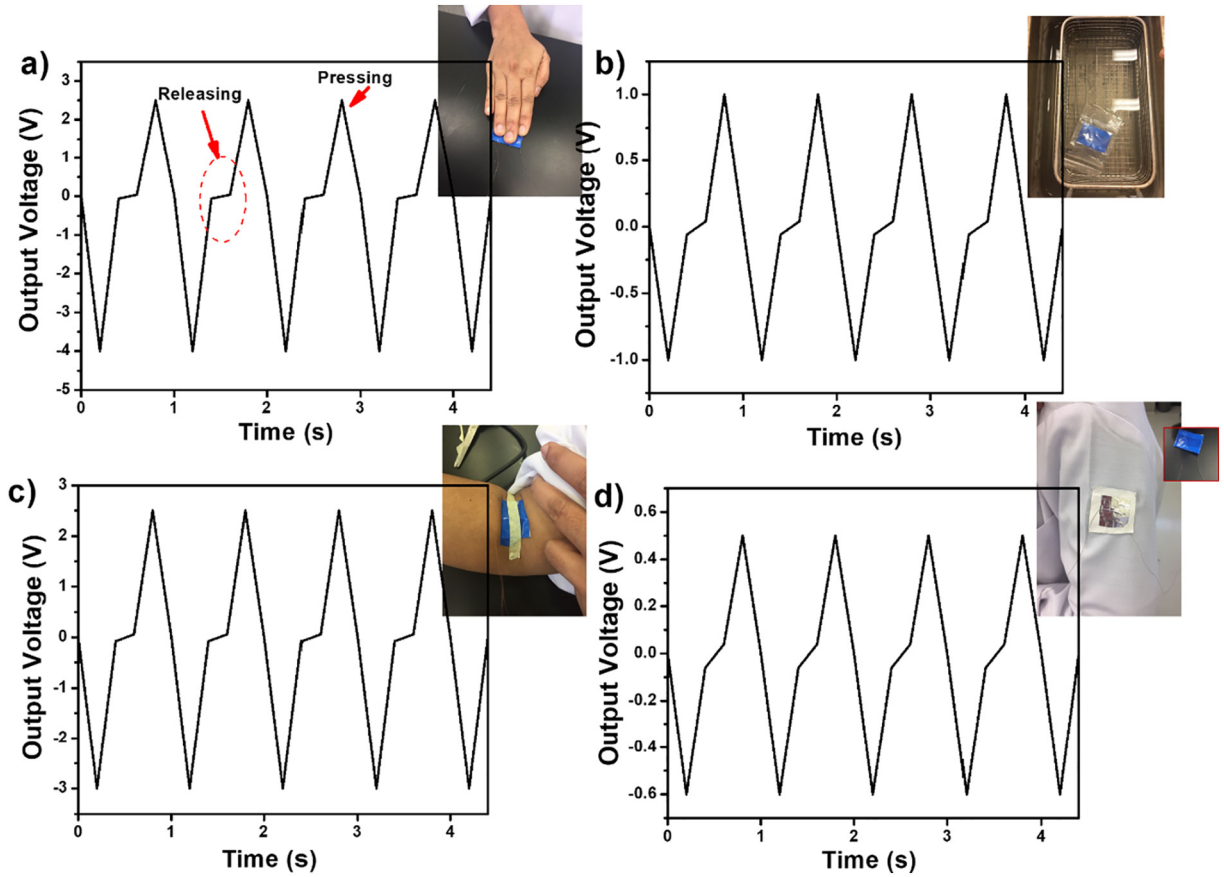

Fig. 4. Variation in output voltage of the PENG with respect to time a) hand tapping b) sonication bath c) elbow movement, d) shoulder movement.

self-powering electronic textiles out of such electrospun fibers. All these testings were repeated for about ten different times and the best results were shown here for the material.

For long-term performance of the PENG, robustness is a key factor required for the nanocomposites, in addition to the flexibility. In order to check the robustness of the spun mats, strain was applied by bending it multiple times [45] as demonstrated in Fig. 5. The piezoelectric property of the samples during bending was checked more than 2000 cycles and the behavior seems to be the same. Fig. 5a and b show the repeatability of the nanocomposite fiber mats in generating the output voltage. The test was performed by keeping the sample in between two stands, of which one is movable and the other is fixed. The movable side moves freely to specific distance in the same way during the whole observed period. The setup is schematically shown in Fig. 5c. The flexibility or the bendable nature of the sample is also demonstrated in the same figure, by showing the image of the sample rolled up on a cylinder. The consistent voltage output establishes the robustness of the hybrid nanocomposite spun membrane and suggest the use of it in practical application without mechanical degradation.

It is interesting to observe the efficiency of PENGs in designing many devices useful for robotics, biomedical sensing, electronic skin designing etc. Moreover, the hybrid nanocomposite fiber possesses better thermal stability, also, as indicated in Fig. S4. The possible mechanism of filler polymer interaction existing in the hybrid [P(VDF-HFP)]/Fe-ZnO-[P(VDF-HFP)]/CNC composite is illustrated in Fig. 5d. The multiple –OH groups on a specific CNC chain form H bonding with oxygen atoms of neighboring chain and this makes the chains standing side by side. This kind of bonding creates electric dipoles spontaneously in the CNC crystal lattice. Each CNC acts as an electric dipole and during compressive stress, the CNC feels a strain and results in strain induced electric polarization. Similar crystalline deformation takes place in the case of Fe-doped ZnO as well, generating dipole moment variations. With external stress, such dipoles undergo displacement. When the force in any form is applied and relaxed, negative and positive charges accumulate at two opposite electrodes and creates piezovoltage. In fact, large positive peak appears due to stress/force and negative peak due to relaxation. When the strain is released the accumulated charges return to opposite direction (reverse polarity) and cancels the voltage. For the hybrid composite, the better filler polymer interaction created the formation of intertwine fibers as evidenced from the TEM images (Fig. 2), and this is the reason for higher piezoelectric activity. In short, the specific advantages of our PENG include cost effectiveness, industrially viable production, lead free piezoelectric power generation and non-toxicity [46].

Dielectric properties of the PVDF nanocomposites are measured from 300 K to 420 K as shown in the Fig. 6. The dielectric constant increases with temperature (Fig. 6a) due to the dipolar polarization taking place within the composites [47]. The dielectric constant of the nanocomposites were higher than that of the neat [P(VDF-HFP)], due to the higher ferroelectric β-phase content in the nanocomposites as well as the interfacial polarization created by the filler materials [48,49]. Room temperature dielectric property variation with frequency for all samples are represented in Fig. S5. Ferroelectric is classified in to dielectric semiconductor normal as it undergoes phase transition with temperature. Such materials exhibit smooth dielectric curves with strong dipole dispersion at high temperature domains [50]. Fig. 6a also shows

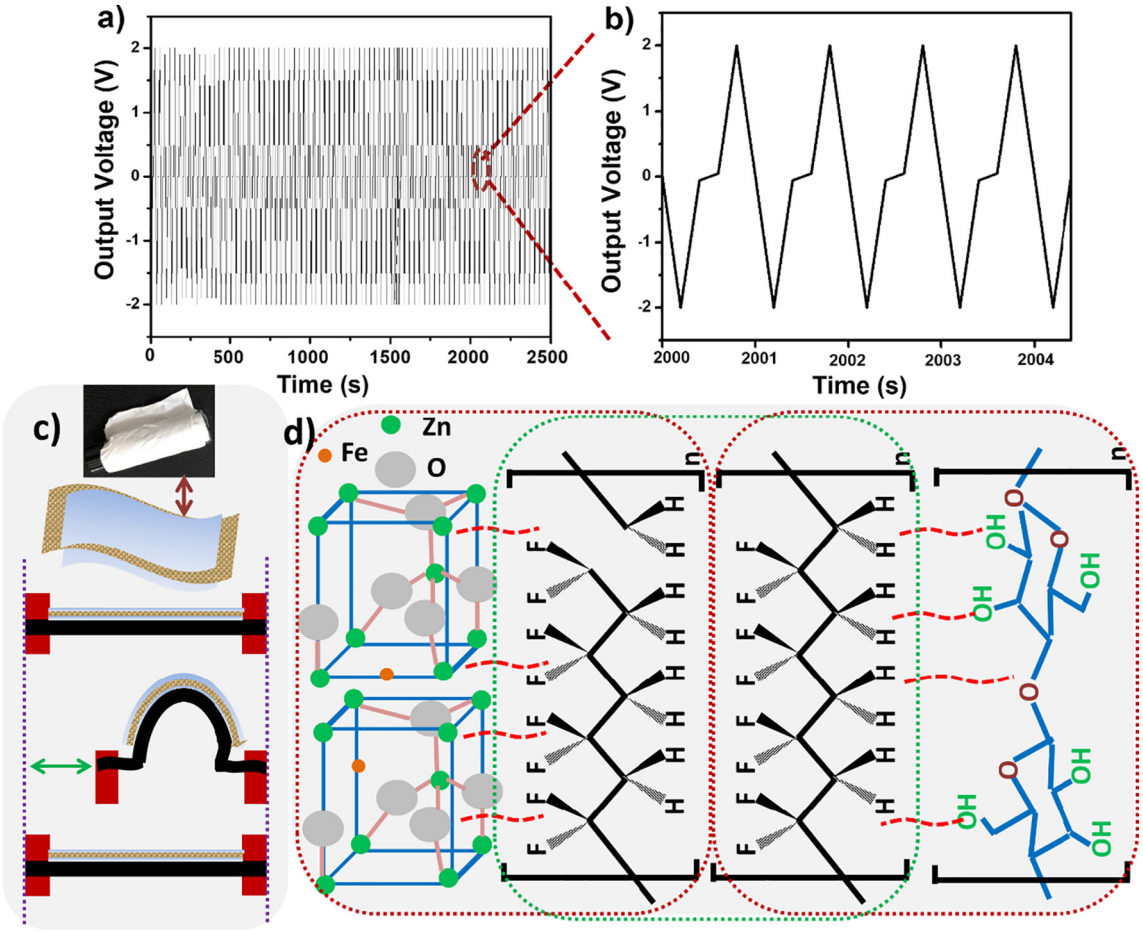

Fig. 5. Variation of piezoelectric output voltage as a function of time for a) long bending cycles b) a few cycles, c) sample flexibility and schematic representation of bending experiment, d) mechanism of interaction existing in the piezoelectric hybrid nanocomposite containing double layers of [P(VDF-HFP)]/Fe-ZnO and [P(VDF-HFP)]/CNC.

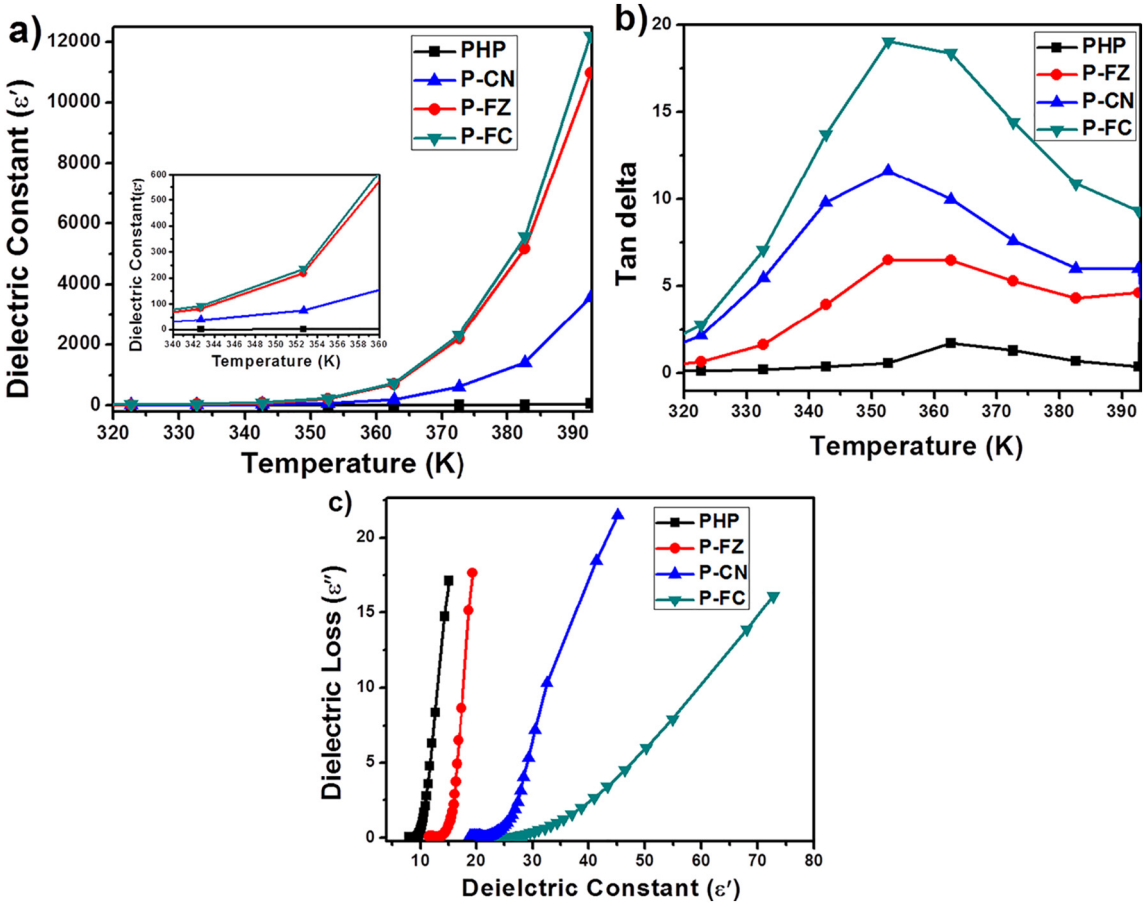

Fig. 6. Dependence of dielectric constant a) and dielectric loss b) on temperature; c) Cole-Cole plots for all samples at room temperature.

a sudden increase in dielectric constant value around 354 K, which is correlated with the Curie temperature. This is also clear in the case of tan δ plots in Fig. 6b. This variation happening at the specific Curie temperature is attributed to the magneto dielectric coupling [51].

Plots of dielectric loss vs constant values clearly identify the structural dynamics of dielectric relaxation process. Such Cole-Cole plots are effective ways to investigate materials with well separated relaxation processes with comparable magnitudes. Many relaxations can occur in a typical nanocomposite, such as due to crystalline regions, charge diffusion and the interphases or defects dispersed in amorphous region [52]. The dipolar reorientation of the polymer chains and the accumulation of filler charge carriers at the interface creates interfacial polarization effect, commonly known as Maxwell-Wagner-Sillars (MWS) relaxation [53,54].

Fig. 6c represents the Cole-Cole plots of various samples investigated here, and represents interesting behavior. It is clear that the plots are deviated from the usual semi-circular Cole-Cole plots, which points out the existence of multiple polarization relaxation mechanisms having various relaxation times. In the ferroelectric [P(VDF-HFP)], numerous nanoscale ordered micro domains exist, as reported [55]. The dielectric behavior of the composite at low frequency is normally due to the conductive nature of composites and at high frequency it is due to the polarization relaxation loss. The relaxation time (τ) is related to the minimum frequency (f_{min}) at which the dielectric loss occurs as explained below.

$$\tau = 1/(2\pi f_{min}) \quad (2)$$

Here the relaxation time calculated for the sample [P(VDF-HFP)]/Fe-ZnO-[P(VDF-HFP)]/CNC was 26.11 μs, much lower than the neat polymer. The relaxation time was also observed to be smaller than our previous report on PVDF containing Fe-doped ZnO synthesized by gamma irradiation [37]. This substantiates the dipole alignment happening within the ferroelectric sample.

Thus, it is worthy to note that the spun membranes of the hybrid nanocomposite are an ideal candidate for harvesting energy to be useful in wearable electronics. It is well clear that the electrospun members can be embedded in normal clothing to ensure mechanical energy harvesting depending on human motion. The superior dielectric properties of the sample also suggest its application in electronic textiles, where the energy storage and energy harvesting equally matter.

4. Conclusions

Unique electrospun membranes as a hybrid layer assembly was made by following simple synthesis routes. The CNC ensured piezoelectric property to the PVDF-HFP polymer, in addition to the ferroelectric Fe-doped ZnO nanomaterials. The typical morphology-rod like CNC and star like Fe-ZnO- other than the nanodimension and high aspect ratio helped in the uniform distribution of nanomaterials within the polymer chains. Weak hydrogen bonding interactions further guaranteed the filler-polymer interfacial compatibility. The hybrid spun membrane was able to generate a maximum of 12 V upon mechanical vibrations, with 5.5 V upon elbow movement and 1.1. V upon cloth folding movement. The compatibility of the membranes on textile materials point towards its possible application in electronic textiles. Moreover, the PENG based on spun fibers produced a power density of 490 μW/cm^3 and exhibited extended durability.

Supplementary data to this article can be found online at https://doi.org/10.1016/j.matdes.2019.108176.

Credit author statement

The first Author DP wrote the entire manuscript by analyzing the data.

The second author, HP and third author, AT were involved with the experimental procedures.

The forth author MAAA supervised the entire work, and did timely reviews and corrections.

Declaration of competing interest

The authors declare no conflict of interest.

Acknowledgement

This publication is made possible by NPRP grant 6-282-2-119 from the Qatar National Research Fund (a member of Qatar Foundation). The statements made herein are solely the responsibility of the authors.

Author contributions

D.P. contributed the research idea, data interpretation and wrote the whole manuscript. H.P. did the experimental works along with A.T. M. A. A. revised the manuscript and supported throughout by timely suggestions and advices. All authors reviewed the manuscript.

Additional information

Competing financial interests: The authors declare no competing financial interests.

References

[1] B. Dutta, E. Kar, N. Bose, S. Mukherjee, NiO@ SiO2/PVDF: a flexible polymer nanocomposite for high performance human body motion based energy harvester and tactile e-skin mechanosensor, ACS Sustain. Chem. Eng. 6 (2018) 10505–10516.
[2] Y. Zhang, C.K. Jeong, J. Wang, H. Sun, F. Li, G. Zhang, L.Q. Chen, S. Zhang, W. Chen, Wang Q. Wang, Flexible energy harvesting polymer composites based on biofibril-templated 3-dimensional interconnected piezoceramics, Nano Energy 50 (2018) 35–42.
[3] Y. Zhang, L. Zhang, K. Cui, S. Ge, X. Cheng, M. Yan, J. Yu, H. Liu, Flexible electronics based on micro/nanostructured paper, Adv. Mat. 30 (51) (2018) (1801588).
[4] S. Varma, K. Sambath Kumar, S. Seal, S. Rajaraman, J. Thomas, Fiber-type solar cells, nanogenerators, batteries, and supercapacitors for wearable applications, Adv. Sci. (2018) 1800340.
[5] D.P. Hansora, N.G. Shimpi, S. Mishra, Performance of hybrid nanostructured conductive cotton materials as wearable devices: an overview of materials, fabrication, properties and applications, RSC Adv. 5 (130) (2015) 107716–107770.
[6] S.K. Ghosh, P. Adhikary, S. Jana, A. Biswas, V. Sencadas, S.D. Gupta, B. Tudu, D. Mandal, Electrospun gelatin nanofiber based self-powered bio-e-skin for health care monitoring, Nano Energy 36 (2017) 166–175.
[7] T.Q. Trung, N.E. Lee, Flexible and stretchable physical sensor integrated platforms for wearable human-activity monitoring and personal healthcare, Adv. Mat. 28 (22) (2016) 4338–4372.
[8] S.K. Karan, R. Bera, S. Paria, A.K. Das, S. Maiti, A. Maitra, B.B. Khatua, An approach to design highly durable piezoelectric nanogenerator based on self-poled PVDF/AlO-rGO flexible nanocomposite with high power density and energy conversion efficiency, Adv. Energy Mat. 6 (20) (2016), 1601016.
[9] W. Zeng, L. Shu, Q. Li, S. Chen, F. Wang, X.M. Tao, Fiber-based wearable electronics: a review of materials, fabrication, devices and applications, Adv. Mat. 26 (31) (2014) 5310–5336.
[10] A. Delnavaz, J. Voix, Flexible piezoelectric energy harvesting from jaw movements, Smart Mat. Struct. 23 (10) (2014), 105020.
[11] H. Parangusan, D. Ponnamma, M.A. Al-Maadeed, Stretchable electrospun PVDF-HFP/Co-ZnO nanofibers as piezoelectric nanogenerators, Sci. Rep. 8 (1) (2018) 754.
[12] A.A. Issa, M.A. Al-Maadeed, A.S. Luyt, D. Ponnamma, M.K. Hassan, Physico-mechanical, dielectric, and piezoelectric properties of PVDF electrospun mats containing silver nanoparticles, Materials C 3 (4) (2017) 30.
[13] X. Chen, X. Li, J. Shao, N. An, H. Tian, C. Wang, T. Han, L. Wang, B. Lu, High-performance piezoelectric nanogenerators with imprinted P(VDF-TrFE)/BaTiO3 nanocomposite micropillars for self-powered flexible sensors, Small 13 (23) (2017) 1604245.
[14] H. Parangusan, D. Ponnamma, M.A. AlMaadeed, Flexible tri-layer piezoelectric nanogenerator based on PVDF-HFP/Ni-doped ZnO nanocomposites, RSC Adv. 7 (79) (2017) 50156–50165.
[15] D. Ponnamma, M.M. Chamakh, K. Deshmukh, M.B. Ahamed, A. Erturk, P. Sharma, M.A. Al-Maadeed, Ceramic-based polymer nanocomposites as piezoelectric materials, in: D. Ponnamma, K.K. Sadasivuni, J.J. Cabibihan, M.A. AlMaadeed (Eds.), Smart Polymer Nanocomposites, Springer, Cham 2017, pp. 77–93.
[16] D. Ponnamma, A. Erturk, H. Parangusan, K. Deshmukh, M.B. Ahamed, M.A. Al-Maadeed, Stretchable quaternary phasic PVDF-HFP nanocomposite films containing graphene-titania-$SrTiO_3$ for mechanical energy harvesting, Emerg. Mat. 1 (1–2) (2018) 55–65.
[17] T.I. Lee, W.S. Jang, E. Lee, Y.S. Kim, Z.L. Wang, H.K. Baik, J.M. Myoung, Ultrathin self-powered artificial skin, Energy & Environmental Sci 7 (12) (2014) 3994–3999.
[18] J. Yang, J. Chen, Y. Liu, W. Yang, Y. Su, Z.L. Wang, Triboelectrification-based organic film nanogenerator for acoustic energy harvesting and self-powered active acoustic sensing, ACS Nano 8 (3) (2014) 2649–2657.
[19] J. Chen, J. Yang, Z. Li, X. Fan, Y. Zi, Q. Jing, H. Guo, Z. Wen, K.C. Pradel, S. Niu, Z.L. Wang, Networks of triboelectric nanogenerators for harvesting water wave energy: a potential approach toward blue energy, ACS Nano 9 (3) (2015) 3324–3331.
[20] J. Ma, U. Azhar, C. Zong, Y. Zhang, A. Xu, C. Zhai, L. Zhang, S. Zhang, Core-shell structured PVDF@ BT nanoparticles for dielectric materials: a novel composite to prove the dependence of dielectric properties on ferroelectric shell, Mater. Des. 164 (2019 Feb 15) 107556.
[21] Z. Pi, J. Zhang, C. Wen, Z.B. Zhang, D. Wu, Flexible piezoelectric nanogenerator made of poly(vinylidenefluoride-co-trifluoroethylene) (PVDF-TrFE) thin film, Nano Energy 7 (2014) 33–41.
[22] P. Sukwisute, J. Yuennan, N. Muensit, Enhancement of ferroelectric phase and dielectric properties of P (VDF-HFP) by NiCl2· 6H2O nucleating agent, Integr. Ferroelectr. 195 (1) (2019) 230–239 Jan 2.
[23] L. Yang, Q. Zhao, Y. Hou, L. Hong, H. Ji, L. Xu, K. Zhu, M. Shen, H. Huang, H. He, J. Qiu, Flexible polyvinylidene fluoride based nanocomposites with high and stable piezoelectric performance over a wide temperature range utilizing the strong multi-interface effect, Compos. Sci. Technol. 174 (2019) 33–41 Apr 12.
[24] D. Ponnamma, M.A. Al-Maadeed, Influence of BaTiO3/white graphene filler synergy on the energy harvesting performance of a piezoelectric polymer nanocomposite, Sustainable energy & fuels 3 (3) (2019) 774–785.
[25] P. Costa, J. Nunes-Pereira, N. Pereira, N. Castro, S. Gonçalves, S. Lanceros-Mendez, Recent progress on piezoelectric, pyroelectric, and magnetoelectric polymer-based energy-harvesting devices, Energy Technology 7 (7) (2019) 1800852–1800862.
[26] D. Singh, A. Choudhary, A. Garg, Flexible and robust piezoelectric polymer nanocomposites based energy harvesters, ACS Appl. Mat. Interf. 10 (3) (2018) 2793–2800.
[27] A. Kumar, H. Gullapalli, K. Balakrishnan, A. Botello-Mendez, R. Vajtai, M. Terrones, P.M. Ajayan, Flexible ZnO–cellulose nanocomposite for multisource energy conversion, Small 7 (15) (2011) 2173–2178.
[28] Z. Li, X. Zhang, G. Li, In situ ZnO nanowire growth to promote the PVDF piezo phase and the ZnO–PVDF hybrid self-rectified nanogenerator as a touch sensor, Phys. Chem. Chem. Phys. 16 (12) (2014) 5475–5479.
[29] S. Jana, S. Garain, S.K. Ghosh, S. Sen, D. Mandal, The preparation of γ-crystalline non-electrically poled photoluminescant ZnO–PVDF nanocomposite film for wearable nanogenerators, Nanotechnology 27 (44) (2016), 445403.
[30] J. Jayachandiran, S. Vajravijayan, N. Nandhagopal, K. Gunasekaran, D. Nedumaran, Fabrication and characterization of ZnO incorporated cellulose microfiber film: structural, morphological and functional investigations, J. Mater. Sci. Mater. Electron. 30 (6) (2019) 6037–6049 Mar 1.
[31] H. Fashandi, M.M. Abolhasani, P. Sandoghdar, N. Zohdi, Q. Li, M. Naebe, Morphological changes towards enhancing piezoelectric properties of PVDF electrical generators using cellulose nanocrystals, Cellulose 23 (6) (2016) 3625–3637.
[32] S. Rajala, T. Siponkoski, E. Sarlin, M. Mettänen, M. Vuoriluoto, A. Pammo, J. Juuti, O.J. Rojas, S. Franssila, S. Tuukkanen, Cellulose nanofibril film as a piezoelectric sensor material, ACS Appl. Mat Interf. 8 (24) (2016) 15607–15614.
[33] M.C. Paganini, A. Giorgini, N.P. Gonçalves, C. Gionco, A.B. Prevot, P. Calza, New insight into zinc oxide doped with iron and its exploitation to pollutants abatement, Catal. Today 328 (2019) 230–234 May 15.
[34] P.K. Sharma, R.K. Dutta, A.C. Pandey, S. Layek, H.C. Verma, Effect of iron doping concentration on magnetic properties of ZnO nanoparticles, J. Magn. Magn. Mater. 321 (17) (2009) 2587–2591 Sep 1.
[35] A. Tanvir, Y.H. El-Gawady, M.A. Al-Maadeed, Cellulose nanofibers to assist the release of healing agents in epoxy coatings, Progress in Organic Coatings 112 (2017) 127–132.
[36] A.C.W. Leung, S. Hrapovic, E. Lam, Y. Liu, K.B. Male, K.A. Mahmoud, J.H.T. Luong, Characteristics and properties of carboxylated cellulose nanocrystals prepared from a novel one-step procedure, Small 7 (2011) 302–305.
[37] P. Hemalatha, D. Ponnamma, M.A. Al-Maadeed, Investigation on the effect of γ-irradiation on the dielectric and piezoelectric properties of stretchable PVDF/Fe-ZnO nanocomposites for self-powering devices, Soft Matter 14 (43) (2018) 8803.
[38] H. Zhu, F. Shen, W. Luo, S. Zhu, M. Zhao, B. Natarajan, J. Dai, L. Zhou, X. Ji, R.S. Yassar, T. Li, Low temperature carbonization of cellulose nanocrystals for high performance carbon anode of sodium-ion batteries, Nano Energy 33 (2017) 37–44.
[39] G. Zhang, Q. Liao, Z. Zhang, Q. Liang, Y. Zhao, X. Zheng, Y. Zhang, Novel piezoelectric paper-based flexible nanogenerators composed of $BaTiO_3$ nanoparticles and bacterial cellulose, Adv. Sci. 3 (2) (2016), 1500257.
[40] Y. Mao, P. Zhao, G. McConohy, H. Yang, Y. Tong, X. Wang, Sponge-like piezoelectric polymer films for scalable and integratable nanogenerators and self-powered electronic systems, Adv. Energy Mater. 4 (2014), 1301624.
[41] V. Bhavanasi, V. Kumar, K. Parida, J. Wang, P.S. Lee, Enhanced piezoelectric energy harvesting performance of flexible PVDF-TrFE bilayer films with graphene oxide, ACS Appl. Mater. Interfaces 8 (2016) 521–529.
[42] G. Zhang, Q. Liao, M. Ma, F. Gao, Z. Zhang, Z. Kang, Y. Zhang, Uniformly assembled vanadium doped ZnO microflowers/bacterial cellulose hybrid paper for flexible

piezoelectric nanogenerators and self-powered sensors, Nano Energy 52 (2018) 501–509.
[43] K. Ghosal, A. Chandra, G. Praveen, S. Snigdha, S. Roy, C. Agatemor, S. Thomas, I. Provaznik, Electrospinning over solvent casting: tuning of mechanical properties of membranes, Sci. Rep. 8 (1) (2018) 5058.
[44] L. Csoka, I.C. Hoeger, O.J. Rojas, I. Peszlen, J.J. Pawlak, P.N. Peralta, Piezoelectric effect of cellulose nanocrystals thin films, ACS Macro Lett. 1 (7) (2012) 867–870.
[45] S.H. Shin, Y.H. Kim, M.H. Lee, J.Y. Jung, J. Nah, Hemispherically aggregated $BaTiO_3$ nanoparticle composite thin film for high-performance flexible piezoelectric nanogenerator, ACS Nano 8 (3) (2014) 2766–2773.
[46] M.M. Alam, D. Mandal, Native cellulose microfiber-based hybrid piezoelectric generator for mechanical energy harvesting utility, ACS Appl. Mater. Interf. 8 (3) (2016) 1555–1558.
[47] C. Thirmal, C. Nayek, P. Murugavel, V. Subramanian, Magnetic, dielectric and magneto dielectric properties of PVDF-La0.7Sr0.3MnO3 polymer nanocomposite film, AIP Adv. 3 (11) (2013), 112109.
[48] K. Deshmukh, M.B. Ahamed, R.R. Deshmukh, S.K. Pasha, K.K. Sadasivuni, A.R. Polu, D. Ponnamma, M.A. AlMaadeed, K. Chidambaram, Newly developed biodegradable polymer nanocomposites of cellulose acetate and Al2O3 nanoparticles with enhanced dielectric performance for embedded passive applications, J. Mat. Sci. Mat. Electron. 28 (1) (2017) 973–986.
[49] D. Ponnamma, M.A. Al-Maadeed, 3D architectures of titania nanotubes and graphene with efficient nanosynergy for supercapacitors, Mat. Des. 117 (2017) 203–212.
[50] S. Abdalla, A. Obaid, F.M. Al-Marzouki, Preparation and characterization of poly (vinylidene fluoride): a high dielectric performance nano-composite for electrical storage, Results in Phys 6 (2016) 617–626.
[51] M.A. Zurbuchen, T. Wu, S. Saha, J. Mitchell, S.K. Streiffer, Multiferroic composite ferroelectric-ferromagnetic films, Appl. Phys. Lett. 87 (23) (2005), 232908.
[52] X. Jiang, X. Zhao, G. Peng, W. Liu, K. Liu, Z. Zhan, Investigation on crystalline structure and dielectric relaxation behaviors of hot pressed poly (vinylidene fluoride) film, Current Appl. Phys. 17 (1) (2017) 15–23.
[53] K. Deshmukh, M.B. Ahamed, K.K. Sadasivuni, D. Ponnamma, M.A. AlMaadeed, R.R. Deshmukh, S.K. Pasha, A.R. Polu, K. Chidambaram, Fumed SiO_2 nanoparticle reinforced biopolymer blend nanocomposites with high dielectric constant and low dielectric loss for flexible organic electronics, J. Appl. Polym. Sci. 134 (5) (2017).
[54] K. Deshmukh, M.B. Ahamed, R.R. Deshmukh, S.K. Pasha, K.K. Sadasivuni, D. Ponnamma, M.A. AlMaadeed, Striking multiple synergies in novel three-phase fluoropolymer nanocomposites by combining titanium dioxide and graphene oxide as hybrid fillers, J. Mat. Sci. Mat. Electron. 28 (1) (2017) 559–575.
[55] X. Liu, S. Liu, M.G. Han, L. Zhao, H. Deng, J. Li, Y. Zhu, L. Krusin-Elbaum, S. O'Brien, Magnetoelectricity in CoFe2O4 nanocrystal-P (VDF-HFP) thin films, Nanoscale Res. Lett. 8 (1) (2013) 374.